

Spatiotemporal Modeling of Swedish Scots Pine Stands

Ottmar Cronie, Kenneth Nyström, and Jun Yu

Abstract: The growth-interaction (GI) process is used for the spatiotemporal modeling of measurements of locations and radii at breast height made at three different time points of the individual trees in 10 Scots pine (*Pinus sylvestris*) plots from the Swedish National Forest Inventory. The GI process places trees at random locations in the study region and assigns sizes to the trees, which interact and grow with time. It has been used to model plots in previous studies and to improve the fit we suggest some modifications: a different location assignment strategy and a different open-growth (growth under negligible competition) function. We believe that the calibration data contain trees that are too small to reflect the open growth properly, which primarily affects the carrying capacity parameter. To better represent the open growth of Scots pines, we evaluate the open growth from a separate set of data (size and age measurements of older and larger single Scots pines). A linear relationship is found between the plot's estimated site indices and the sizes, and this is exploited in the estimation of the carrying capacity. We finally estimate the remaining GI process parameters and test the goodness of fit on simulated predictions from the fitted model. FOR. SCI. 59(5):505–516.

Keywords: goodness of fit, open growth, Richards growth function, Scots pines, spatiotemporal point process

FOR A LONG TIME, STATISTICAL METHODS for (marked) spatial point processes have been used extensively to determine various characteristics of forest stands (cf. Diggle 2003, Stoyan and Penttinen 2000, Illian et al. 2008 for general surveys and Grabarnik and Särkkä 2009 for a specific study). For instance, different summary statistics, such as Ripley's K function (Illian et al. 2008, p. 214), have been able to depict the inherent mechanisms that govern the way individual trees are located spatially. In addition, the temporal development of the sizes of individual trees has also been explicitly modeled (Shifley and Brand 1984, Zeide 1993). Note, however, that when considering different spatial features of a forest stand at a fixed time, we are in fact, to some extent, also considering the temporal development of each individual tree which has been present up to the current time point. Put differently, we always regard some aspect of the spatiotemporal development of all the trees when we consider either just one single tree or when we consider all the trees in the whole stand. Hence, if one wants a deeper understanding of the inherent growth process that governs the growth of individual trees in a forest stand, it is reasonable to instead extend the study to consider the full spatiotemporal development of the stand, because the spatial domain and the temporal domain clearly are intertwined (Gratzer et al. 2004).

Our main objective here is to describe the development of young Scots pine stands in Sweden. The specific approach chosen here is to fit the so-called growth-interaction (GI) process (Särkkä and Renshaw 2006, Cronie and Särkkä 2011) to a collection of data sets. More specifically, each data set under consideration consists of measurements of

individual trees in a single Scots pine stand at a few different time points. For each individual tree, we have recorded its location as well as its radius at breast height (rbh) (1.3 m aboveground) at all measurement times of the stand. It should be pointed out that in the remaining parts of the article, rbh is used to describe tree size rather than the more common dbh ($\text{dbh} = 2 \text{rbh}$). This choice is made partly out of mathematical convenience and partly because the GI process (and in particular its spatial interaction structure) has a more natural interpretation when the marks describe radial growth.

The GI process is a spatiotemporal marked point process in which new points (trees) arrive to the study region at random times and receive random locations in the study region. Once they arrive they also receive sizes (radii of disks centered on their locations) and start growing and competing until they finally die, either by competition or naturally. Because we are modeling rbh, at a given time point such a disk represents the breast height area $[\pi(\text{rbh})^2]$ occupied by the tree at that time.

A previous (initial) study similar to the current one was conducted by Cronie and Särkkä (2011), in which the GI process was used to model one Scots pine data set of the same type as the data sets considered here. It was indicated that the GI process is an appropriate model for such data. However, simulated point patterns of the GI process, which were generated based on the parameter estimates obtained by fitting the GI process to the data, had nearest neighbor distances that were smaller than what was observed in the actual data. Furthermore, the estimated open growth, i.e., the growth of a tree when the competition with other trees

Manuscript received February 4, 2012; accepted September 3, 2012; published online November 15, 2012; <http://dx.doi.org/10.5849/forsci.12-007>.

Ottmar Cronie (ottmar@alumni.chalmers.se), Mathematical Sciences, Chalmers University of Technology and University of Gothenburg. Kenneth Nyström (kenneth.nystrom@slu.se), Department of Forest Resource Management, Swedish University of Agricultural Sciences. Jun Yu (jun.yu@math.umu.se), Department of Mathematics and Mathematical Statistics, Umeå University, Umeå, Sweden.

Acknowledgments: We are grateful for useful comments and suggestions from Aila Särkkä and want to thank one associate editor and two reviewers for their valuable comments and constructive suggestions. This research has been supported by the Swedish Research Council and the Swedish Foundation for Strategic Research.

Copyright © 2013 by the Society of American Foresters.

is negligible, suggested that after approximately 40 years (in open growth), a Scots pine had reached its theoretical maximal attainable size—its carrying capacity. Empirical observations on inventory plots revealed that Scots pine exceed a biologically maximal size later in Sweden (Figure 2). In addition, the observed size distributions in the data and in the simulations were different. The suggested remedy was to change the form of the open-growth function in the model, which controls the growth of a tree in the absence of competition in the model, to a more flexible one. In addition, a more realistic setting to assign the locations to the new trees in the model may improve the fit of the model. More specifically, instead of letting the location of a new tree be uniformly distributed in the whole study region, as was previously the case (Särkkä and Renshaw 2006, Cronie and Särkkä 2011), in the present study, we let the location of the tree be uniformly distributed on the part of the study region which is not already occupied by the other trees present at its arrival time. Note that this is a natural assumption because trees do not grow inside each other.

As mentioned previously, the carrying capacity, denoted by K , is one of the parameters in the GI process that governs the rate of the so-called open growth of a tree in the model. By looking closer at the carrying capacity estimates obtained in Cronie and Särkkä (2011), we believe that the actual carrying capacity was underestimated because the forest stand considered was so young. Because biased carrying capacity estimates result in biased estimates of the open-growth behavior, it is important to obtain fairly adequate estimates of K if we wish to say something about the individual growth ability of a tree (Shifley and Brand 1984). Because the data sets we consider in this study also only contain quite young trees, we base the estimation of the carrying capacity on a completely separate set of data that contains older trees—the open-growth data set. We point out that the stands in both data sets grow in different regions of Sweden, and it is most unlikely that they follow the exact same underlying growth patterns. In particular, the site fertility differs between stands, and we would like to account for such variation between the stands. The approach suggested here is to let the carrying capacity be expressed through the *site productivity index* SI, which is expressed as expected dominant height at 100 years total age, and in the current data sets it has been estimated according to Hägglund and Lundmark (1977). The open-growth data set contains measurements made from a large number of Scots pine stands at one given time point, and each measurement consists of three parts: the size (rbh) of the largest tree, the age of the largest tree, and the stand's SI value. We assume that such a data set reflects the open-growth behavior fairly well because by considering the largest tree in a stand we most likely consider the tree in the stand that has been subject to the least amount of competition. In Renshaw and Comas (2009), a separate estimation of the carrying capacity has already been considered for the GI process, and a fixed value of 0.25 m rbh for the carrying capacity parameter was applied.

This article is structured in the following way. A presentation of the two data sets is given in the next section,

followed by a section in which the GI process is defined. Thereafter, in the subsequent section, the estimation approach for the open growth is presented and the estimation approach for the GI process is recalled, and then the estimation results are presented. Finally, the goodness of fit of predictions of the model is evaluated, followed by some conclusions and discussion.

Data Sets

In this article, two sets of data are considered, the *space-time data set* and the *open-growth data set*. Both are taken from the Swedish National Forest Inventory (NFI). The NFI is an annual sparse stratified sample plot inventory with partial replacement (Ranneby et al. 1987).

Space-Time Data

The space-time data set, modeled by the GI process, consists of permanent sample plots (radius 10 m), which were established between 1983 and 1987 and remeasured for the first time after 5 years, i.e., between 1988 and 1992. About half of the sample was then remeasured a second time between 1993 and 1997. However, from 1994 on the reinventory interval was altered to 6 years. Registrations consist of stand, site, and tree variables (Söderberg 1997). For all trees on the plot with a dbh of at least 10 cm, tree species, rbh/dbh, and position (with coordinates) were measured, whereas smaller trees were registered on a reduced plot and mapped only for a few trees. Sample trees were selected from calipered trees with probabilities given by their basal area. In addition, on sample trees, height, crown height, and cause of damage were also registered.

In the present study, 10 stands (plots) established in 1985 were used for the fitting of the GI process, with data from 1985, 1990, and 1996. Note that the years of measurements are the same for all 10 plots, but the ages (sample times), $T_{j,1}$ (1985), $T_{j,2}$ (1990), and $T_{j,3}$ (1996), $j = 1, \dots, 10$, of the 10 plots at the measurement times differ. In addition, a subsample of these plots (5 plots) remeasured a fourth time, $T_{j,4}$ (2005), was used to evaluate the model.

Each plot considered primarily consists of Scots pines (at least 90%) and contains at least 10 trees. It should be noted that the plots considered are quite young (Table 1) and because only trees with a radius of at least (rbh) 0.05 m are

Table 1. Information about the data sets $\times j, j = 1, \dots, 10$.

j	SI	$T_{j,1}$	$T_{j,2}$	$T_{j,3}$	$n_{T_{j,1}}$	$n_{T_{j,2}}$	$n_{T_{j,3}}$
1	13	23	28	34	15	21	29
2	14	22	27	33	13	26	43
3	16	45	50	56	12	15	17
4	17	30	35	41	2	15	23
5	21	29	34	40	27	45	50
6	19	32	37	43	24	36	48
7	18	25	30	36	34	39	40
8	20	23	28	34	40	51	52
9	14	45	50	56	11	14	16
10	15	45	50	56	9	15	15

SI, site index; $T_{j,k}$, $k = 1, 2, 3$, k th inventory time (stand age, years); $n_{T_{j,k}}$, number of trees that are alive at time $T_{j,k}$.

considered, we restrict our study to the modeling of Scots pines larger than 0.05 m rbh at early ages. Note that a plot may contain trees that are not Scots pines, and we have chosen to include the nonpine trees in the modeling because they affect the spatial structure of the plot as well as its temporal development. In Figure 1 an example of a data set is shown. Here all tree radii have been scaled by a factor of 10 for increased visibility.

Regarding our notation, the circular spatial study region of radius 10 m is denoted by W , and the three sample time points at which the plot has been measured (ages in 1985, 1990, and 1996) are denoted by $T_{j,1}, T_{j,2}, T_{j,3}$. Furthermore, the j th data set is denoted by $\mathbb{X}_j = (\mathbb{X}_j(T_{j,1}), \mathbb{X}_j(T_{j,2}), \mathbb{X}_j(T_{j,3})), j = 1, \dots, 10$, and at each time point $T_{j,k}$ we have that $\mathbb{X}_j(T_{j,k}) = \{(\mathbf{x}_i, m_{ik})\}$, where \mathbf{x}_i and m_{ik} denote the i th tree's location and rbh, respectively. Denote by $n_{T_{j,k}}$ the number of trees that are alive at time $T_{j,k}$. Besides the information given in \mathbb{X}_j , a value of the site index SI is also attached to each plot. Note that for some plots we have measurements $\mathbb{X}_j(T_{j,4})$ from an additional time point $T_{j,4}$, used to evaluate predictions of the fitted GI process. Some plot characteristics are given in Table 1.

Open-Growth Data

Provided that two trees in a forest are close enough to each other, they will compete for resources (e.g., light and nutrients). However, if the distance between them is large enough, their competition becomes negligible. This type of growth, i.e., growth without competition/interaction, is often referred to as *open growth*, and it is often modeled by means of growth functions (Seber and Wild 1989, p. 325, Smith et al. 1992, Prévosto et al. 2000, Vospernik et al. 2010).

When we model the growth of trees, one major part is to model the open-growth characteristics and to estimate the theoretical maximal attainable size—the *carrying capacity*. However, because the plots in the space-time data set contain only fairly young trees, which have not reached their full sizes, these plots do not reflect the potential open growth of Scots pines.

Hence, we choose to gain information about the open-growth relationships of Scots pines from a separate set of data. This data set, which consists of 2,579 plots, is based on data collected in the NFI during 2003–2007, and each plot in the data set contains only Scots pines. The open-growth data set has a wide distribution of tree and stand level characteristics, i.e., SI and tree age (Figure 2); therefore, it contains trees that have larger sizes and higher ages than the trees in the space-time data set and thus better reflects the open-growth scenario. Furthermore, we note that one of the main components of the GI process is a growth function that controls the open growth of the radii. Hence, in modeling of the GI process it is essential that we are able to create a good estimate of the open growth of the pine trees (Shifley and Brand 1984, Vospernik et al. 2010).

Each observation in the open-growth data set $\{(y_j, t_j, SI_j)\}$ comes from a pure Scots pine plot, which has been measured at one time point. Specifically, SI_j denotes the SI value of the j th plot, t_j denotes the age (year) of the largest tree present in the j th plot, and y_j denotes the largest tree's rbh (meters). In addition, some initial filtering has to be performed in the open-growth data to ensure that we are considering trees that have been subject to as little competition as possible. Observations corresponding to the largest 1% and the smallest 1% of the ratios $\{y_j/t_j\}$ were removed. This is done because too large or too small values of y_j/t_j imply that measurement errors are likely to be present. Next, the remaining observations were grouped by age, so that all trees that have the same age are in the same group. Then, in each age group, observations corresponding to the largest 2.5% and the smallest 2.5% of the ratios $\{y_j/t_j\}$ were removed. As a result we have $n = 2,465$ observations $\{(t_j, SI_j, y_j)\}_{j=1}^n$, where $10 \leq SI_j \leq 28$ and $6 \leq t_j \leq 293$. It should further be pointed out that there is some uncertainty present in the SI values assigned to each plot/tree.

In Figure 2 it can be seen that the size development y over time (age) t resembles the typical shape of a growth curve model (Seber and Wild 1989, p. 325). It may further be observed that there tends to be a linear relationship between the maximal attainable size y and the site index SI.

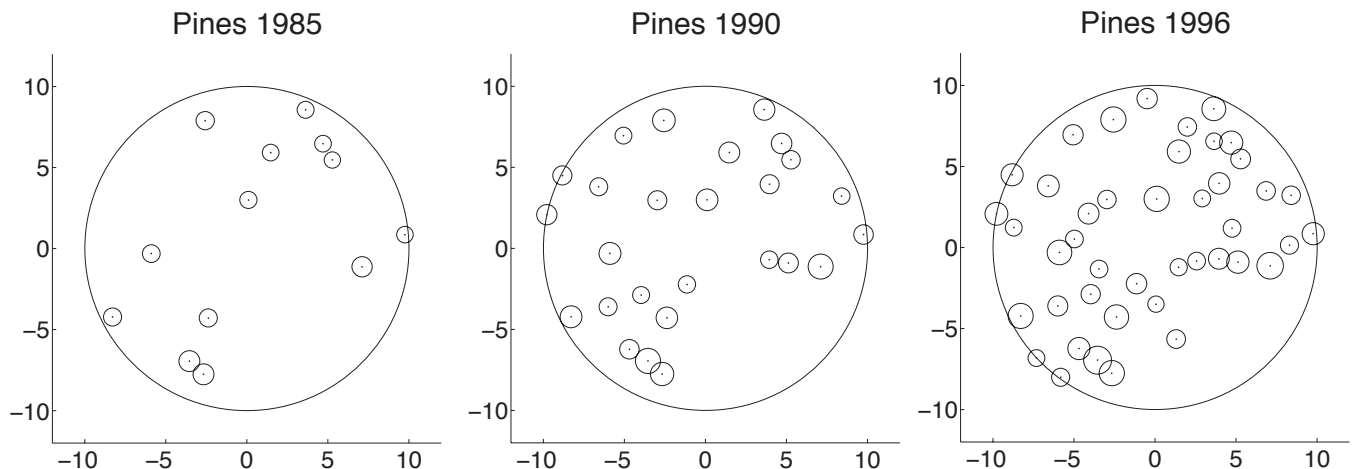


Figure 1. Swedish Scots pine plot recorded in 1985 (left), 1990 (center), and 1996 (right). The radii of the pines are scaled by a factor of 10.

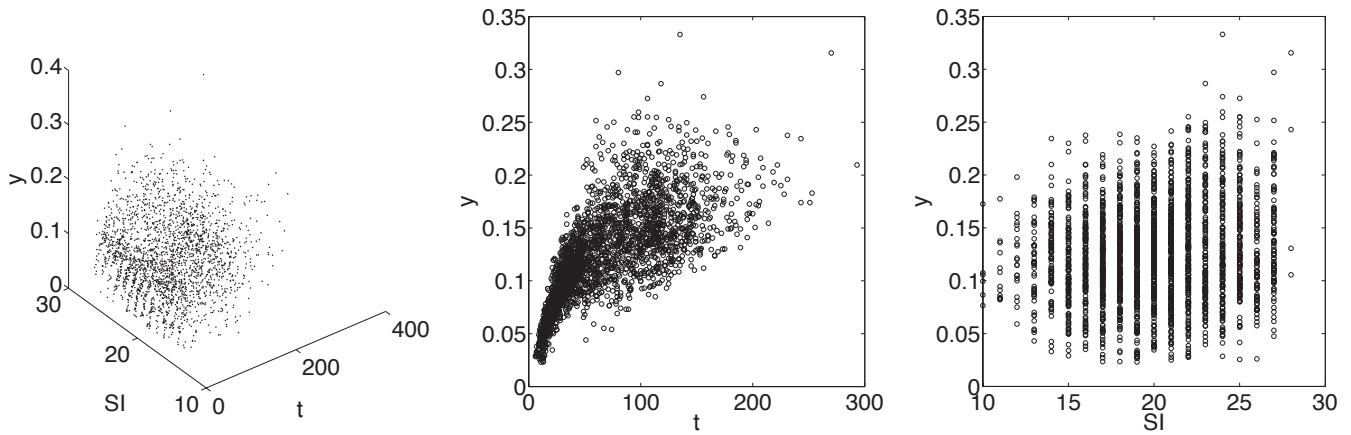


Figure 2. The open-growth data set: $\{(t_j, SI_j, y_j)\}_{j=1}^n$ (left), $\{(t_j, y_j)\}_{j=1}^n$ (center), and $\{(SI_j, y_j)\}_{j=1}^n$ (right). For the largest tree of plot j , y_j , t_j , and SI_j denote the rbh (meters) of the tree, the age (years) of the tree, and the value of the site index SI of the j th plot, respectively.

The GI Process

Consider the scenario in which a plot is measured at the time points $0 < T_1 < \dots < T_n = T$ within a study region W of size $\nu(W)$. Recall that in the current study, W is given by a circular region. As a model for its spatiotemporal development we suggest the so-called growth-interaction process (Särkkä and Renshaw 2006, Comas 2009, Renshaw and Comas 2009, Cronie and Särkkä 2011).

In the GI process, the arrivals of new trees (points) to W occur according to a Poisson process on $[0, T]$ with rate $\alpha\nu(W)$, $\alpha > 0$. At their arrival times $B_1 < \dots < B_N$, the N trees that arrive during $[0, T]$ are assigned the locations (stock centers) X_1, \dots, X_N on W .

The size/radius (rbh) of the i th tree at time $t \in [0, T]$ is denoted by $M_i(t)$, and because we only observe the trees once their radii have reached a certain size (recall that our modeling data consists of trees of at least 0.05 m rbh), we let $M_i(t) = 0$ for all $t < B_i$ and assign the initial size $M_i(B_i) = M_0 > 0$ to the i th tree. As time evolves, the radii $\{M_i(t)\}_{i=1}^N$ will grow and interact with each other. Given that the i th tree has size $M_i(t)$ at time t , its size change over the (infinitesimal) time interval $(t, t + dt)$ is given by

$$M_i(t + dt) = M_i(t) + dM_i(t) \quad (1)$$

$$= M_i(t) + \left(f(M_i(t); \theta) - \sum_{j=1, j \neq i}^N h(M_i(t), M_j(t), X_i, X_j; \theta) \right) dt,$$

where θ is a parameter vector which controls the growth and interaction pattern of the model and $f(\cdot)$ is the growth function that governs the open growth of the i th tree. The function $h(\cdot)$ is the spatial interaction function that handles the spatial pairwise interaction/competition of the i th tree with the other (neighboring) trees.

In accordance with Comas (2009) and Cronie and Särkkä (2011), a tree can also experience a (size-dependent) *natural death*: given $M_i(t)$, the (infinitesimal) probability that the i th tree suffers a natural death during the time interval $(t, t + dt)$ is given by $\mu/(1 + M_i(t)) + o(dt)$, where $\mu > 0$ and $o(dt)$ is some function such that $\lim_{dt \rightarrow 0} o(dt)/dt = 0$ (equivalent interpretation: at each time t the potential remaining lifetime

of the i th tree is $\text{Exp}(\mu/(1 + M_i(t)))$ -distributed). Hereby a tree becomes more viable as it grows in size.

In addition, the competition for resources may cause a tree to die, and we say that the i th tree has suffered a *competitive death* if $M_i(t) \leq 0$ at some time $t > B_i$. Note that hereby the death time of the i th tree is given by the smallest of the natural death time and the competitive death time, and we let $M_i(t) = 0$ once the tree has died.

Returning to the locations of the trees, let the location X_i of the i th tree be uniformly distributed on the part of W , which is not occupied by other (the previous) trees at time $t = B_i$, i.e., $X_i \sim \text{Uni}(W \setminus \cup_{j=1}^{i-1} B_{X_j}[M_j(B_i)])$, where the closed disk $B_{X_j}[M_j(t)]$, with centre X_j and radius $M_j(t)$, represents the (breast height) space which is occupied by the j th tree at time t . Note that we hereby avoid pairs of points that are too close to each other (trees do not grow inside each other). Hence, this approach differs from the earlier arrival strategy, for which the locations are uniformly distributed on the whole W (Särkkä and Renshaw 2006).

Many options are available for $h(\cdot)$ (Nord-Larsen 2006, Särkkä and Renshaw 2006, Renshaw et al. 2009), and we here follow, among others, Särkkä and Renshaw (2006) by using the nonsymmetric (large trees influence small trees more than small trees influence large trees) *area interaction function* (Gerrard 1969)

$$h(M_i(t), M_j(t), X_i, X_j; \theta) = c \frac{\nu(B_{X_i}[rM_i(t)] \cap B_{X_j}[rM_j(t)])}{\nu(B_{X_i}[rM_i(t)])}, \quad (2)$$

where $\nu(B_{X_i}[rM_i(t)])$ denotes the size of the closed disk $B_{X_i}[rM_i(t)]$ and the elements $c \geq 0$ and $r \geq 1$ of the parameter vector θ are referred to as the *force of interaction* and the *scale of interaction*, respectively. $B_{X_i}[rM_i(t)]$, representing the region in which the tree competes for resources, is referred to as the *influence zone* of the i th tree at time t (Weiner and Damgaard 2006). Note that the ratio on the right hand side of expression 2 is the proportion of the i th influence zone that is covered by the j th influence zone at time t . If the distance $\|X_i - X_j\|$ between the i th tree and the j th tree is larger than $rM_i(t) + rM_j(t)$, their influence zones

do not overlap, whereby no interaction takes place between them during $(t, t + dt)$.

As mentioned previously, the *open/individual growth function* $f(M_i(t); \theta)$ in expression (1) controls the growth of a tree in the absence of competing neighboring trees. In the case of no interaction, i.e., when $h(\cdot) = 0$, expression (1) turns into the equation $dM(t)/dt = f(M(t); \theta)$, $M(0) = M_0$, which has $M(t)$ as its solution (for simplicity, we here write $M(t)$ for $M_i(t)$). In the literature, many applications of different growth functions can be found (Seber and Wild 1989, p. 325, Zeide 1993). In the present study, we apply the so-called Richards growth function (RGF) (Seber and Wild 1989, p. 332, Lei and Zhang 2004, Renshaw et al. 2009),

$$M(t) = K(1 + ((M_0/K)^\delta - 1)e^{-\lambda t})^{1/\delta}, \quad (3)$$

where $\delta \neq 1$, $K > 0$, and $\lambda > 0$ (all are elements of the parameter vector θ). Note that this strictly increasing functions is a flexible growth function and through it other growth functions may be derived (Seber and Wild 1989, p. 332, Lei and Zhang 2004), thus largely motivating its use here. For instance, by setting $\delta = -1$ in (3), we obtain the so-called logistic growth function, which has previously been evaluated in the context of the GI process (Särkkä and Renshaw 2006, Renshaw et al. 2009, Cronie and Särkkä 2011). In the RGF, the parameter K is the *carrying capacity* (theoretical upper bound), whereas λ and δ control the growth rate/speed of $M(t)$.

Besides the RGF, there are many good functions for modeling open growth of trees, and one example of such a model is the so-called Weibull growth function (Seber and Wild 1989, p. 337). In Cronie et al. (2011), one can find the open growth analysis performed in this article with the RGF as well as with the Weibull growth function and the logistic growth function; the performance of the Weibull model is almost identical to that of the RGF and it is slightly worse for the logistic model.

Estimation

Estimation of the Open Growth

Recall the open-growth data set $\{(t_j, \text{SI}_j, y_j)\}_{j=1}^n$, $n = 2,465$, from the open-growth data section and also the

observed linear relationship between the maximal attainable size and the site index SI (Figure 2). We argue that because the carrying capacity K tells us how large a tree is allowed to become, it seems sensible to let K be reflected by the fertility, i.e., the site index SI. This linear relationship becomes even more clear in Figure 3, when the observations are divided into groups based on their SI values, for three quantiles $q_\alpha(\text{SI})$, $\alpha = 0.95, 0.975, 0.99$, of the y_j values in each SI group.

The tree size increases with time and therefore, when α is large, $q_\alpha(\text{SI})$ will only be concerned with the older trees in the SI group (Figure 2). Furthermore, the group with SI value 28 only contains four measurements and the largest rbh is 0.3155, which explains why $q_\alpha(28)$ becomes quite extreme (Table 2). When ignoring $q_\alpha(28)$ and fitting linear regression models, we obtain $q_{0.95}(\text{SI}) = 0.1353 + 0.0033 \text{ SI}$, $q_{0.975}(\text{SI}) = 0.1365 + 0.0040 \text{ SI}$, and $q_{0.99}(\text{SI}) = 0.1305 + 0.0051 \text{ SI}$. All three linear trends (intercept and slope) are significant at the 0.05 significance level, and qq plots together with Lillie tests (H_0 : data are Gaussian; H_1 : data are non-Gaussian) suggest that the residuals are normally distributed (Lillie test P values: $P_{0.95} = 0.2082$, $P_{0.975} = 0.0987$, and $P_{0.99} > 0.5$). Thus, it is concluded that there is some linear relationship between SI and K .

The usual approach to fitting a growth curve model to size measurements made over time is to fit the (nonlinear) regression model $Y_j = M(t_j; \theta) + \varepsilon_j$ to the time-size measurements (t_j, Y_j) , $j = 1, \dots, n$, where $M(t_j; \theta)$ is a growth function and the ε_j 's are i.i.d. random variables with mean 0 and variance σ^2 . By accepting the linear relationship $K = a_0 + a_1 \text{ SI}$ for the upper bound of the rbh, we suggest the following regression model

$$Y_j = M(t_j; K, \lambda, \delta) + \varepsilon_j = M(t_j; a_0 + a_1 \text{SI}_j, \lambda, \delta) + \varepsilon_j, \quad (4)$$

where $M(t; \cdot)$ is given by the RGF.

Before the growth curve model (4) is fitted to the open-growth data, the three first SI groups as well as the last two SI groups are merged because there is some uncertainty present in the SI values and some of the SI groups are too small. The new SI values assigned to the new groups are obtained in the following way. We take a weighted mean of

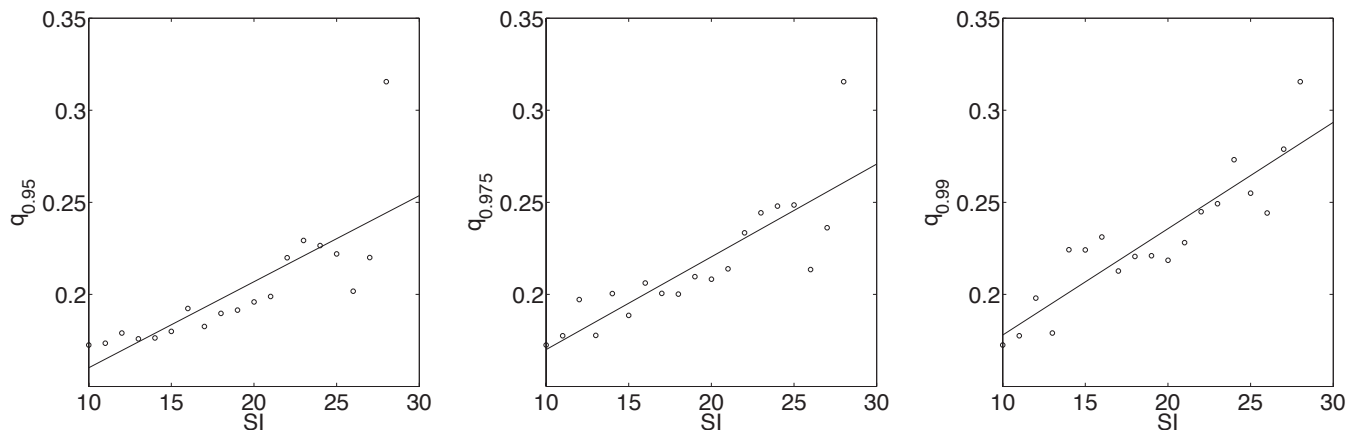


Figure 3. Fitted linear regressions with respect to the pairs $(\text{SI}, q_\alpha(\text{SI}))$. Left, $\alpha = 0.95$; center, $\alpha = 0.975$; and right, $\alpha = 0.99$.

Table 2. Information about each SI group.

SI	n	$\max y_j$
10	6	0.1725
11	12	0.1775
12	21	0.1980
13	45	0.1790
14	92	0.2345
15	123	0.2300
16	154	0.2375
17	210	0.2190
18	207	0.2385
19	254	0.2350
20	232	0.2270
21	246	0.2415
22	216	0.2550
23	157	0.2865
24	156	0.3330
25	153	0.2725
26	87	0.2525
27	90	0.2970
28	4	0.3155

n , number of observations in the group; $\max y_j$, size of the largest tree in the group.

the SI values of the included (old) SI groups, and the weights are determined by the number of observations in each of the SI groups included. More specifically, by merging the SI groups 10, 11, and 12, the new group SI_{10-12} results, which has SI value $(6 \cdot 10 + 12 \cdot 11 + 21 \cdot 12)/(6 + 12 + 21) = 11.3846$ (Table 2). Furthermore, by merging the SI groups 27 and 28, we obtain the new group SI_{27-28} which has SI value $(90 \cdot 27 + 4 \cdot 28)/(90 + 4) = 27.0426$. Note that the number of observations in the groups SI_{10-12} and SI_{27-28} are 39 and 94, respectively. Considering these new SI groups, the results after fitting the regression model 4 to the open-growth data set can be found in Table 3.

The corresponding (normal) qq plot of the residuals is given in Figure 4 and indicates that the residuals are not normally distributed. In addition, the variance increases with the size of \hat{y}_j or, equivalently, the variance grows with increasing t_j (since $M(t; \cdot)$ is an increasing function). Possibly a more accurate model is to consider a multiplicative error, i.e., $Y_j = M(t_j; a_0 + a_1 SI_j, \lambda, \delta)\varepsilon_j$. However, because we are mainly concerned with the estimation of K , the specification of the error term is of less importance to us. Note that we obtain $\hat{K}|SI_{10-12} = 0.13730$ and $\hat{K}|S_{27-28} = 0.22412$, which both are much lower than the observed maximum radii.

Estimation of the Carrying Capacity

To further explore the estimation of K , we now compare the estimates $\hat{K} = \hat{a}_0 + \hat{a}_1 SI$ in Table 3 with the three linear regressions $\hat{K} = q_\alpha(SI) = b_0 + b_1 SI$, $\alpha = 0.95, 0.975, 0.99$, which are based on the α quantiles of each (new) SI group. The results obtained can be found in Table 4 and just as

Table 3. Results after fitting of the regression model 4 to the open-growth data set.

\hat{a}_0	\hat{a}_1	\hat{M}_0	$\hat{\lambda}$	$\hat{\delta}$
0.07418	0.00554	$6.5 \times 10^{-253} (\approx 0)$	0.01752	1.29434

before the linear relationship is significant in each case, and the residuals can be assumed to be normally distributed (Lillie test P values: $P_{0.95} > 0.5$, $P_{0.975} = 0.0587$, and $P_{0.99} = 0.3147$).

We thus conclude that, for all SI values, the maximal attainable size of a tree suggested by $\hat{K} = q_\alpha(SI) = \hat{b}_0 + \hat{b}_1 SI$ is larger than the maximal attainable size suggested by the (growth function) estimate of K in Table 3. For SI_{10-12} the largest y_j values reach approximately 0.2 and for SI_{27-28} they reach approximately 0.3 (Table 2); therefore, it seems more reasonable to use, e.g., $\alpha = 0.975$ when we employ $q_\alpha(SI) = \hat{b}_0 + \hat{b}_1 SI$ to estimate K . Note that we do not use $\alpha = 0.99$ because extreme values in the data may contain measurement errors. This choice of α corresponds, more or less, to the fixed estimate $\hat{K} = 0.25$ used in Renshaw et al. (2009), which was motivated by the study conducted in Pukkala et al. (1994). In Table 5, we find the estimates obtained after plugging $\hat{K} = q_{0.975}(SI) = 0.12920 + 0.00441 SI$ into the RGF and, subsequently, estimated the remaining parameters, as explained in the open-growth estimation section.

Estimation of the GI Process Parameters

Having estimated K separately by $\hat{K} = q_{0.975}(SI) = 0.12920 + 0.00441 SI$, we now turn to the space-time data and the estimation of the remaining parameters, i.e., $\theta^* = (\lambda, \delta, c, r), \mu$, and α . The estimation approach used previously to fit the GI process to space-time data was first introduced in Särkkä and Renshaw (2006), and in Cronie and Särkkä (2011) it was adjusted to accommodate the size-dependent natural deaths. It consists of two separate parts: the arrival and death rates α and μ are estimated using a maximum likelihood (ML) estimation procedure, whereas the growth and interaction parameters θ are estimated (separately) through a least-squares scheme. In the case of θ , we here follow the approach suggested in Cronie and Särkkä (2011), with the exception that we use the estimate $\hat{K} = q_{0.975}(SI)$ for the carrying capacity and estimate θ^* by means of the least-squares approach.

In order to obtain the estimates $\hat{\theta}^* = (\hat{\lambda}, \hat{\delta}, \hat{c}, \hat{r})$ for a given data set \mathbb{X}_j , we minimize the sum of squared differences

$$S(\theta^*) = \sum_k \sum_i (\tilde{m}_{ik}(\theta^*, \hat{K}) - m_{ik})^2$$

between the predicted (model-based) sizes $\tilde{m}_{ik}(\theta^*, \hat{K})$ and the observed sizes m_{ik} .

The first sum is taken over sample time points, and the second sum is taken over all trees that are alive at a specific sample time point. In finding $\hat{\theta}^*$, we have to rely on some numerical minimization routine to minimize the sum of squares $S(\theta^*)$, and we here choose to use the same Markov chain Monte Carlo type of method as was used in Cronie and Särkkä (2011) (more details are given in Cronie 2010). In addition, because there are no observations available outside the study region W , some approach to impede the consequences of the so-called edge effects is needed (Illian et al. 2008, p. 180). Three spatiotemporal edge correction methods presented in the context of the GI process were

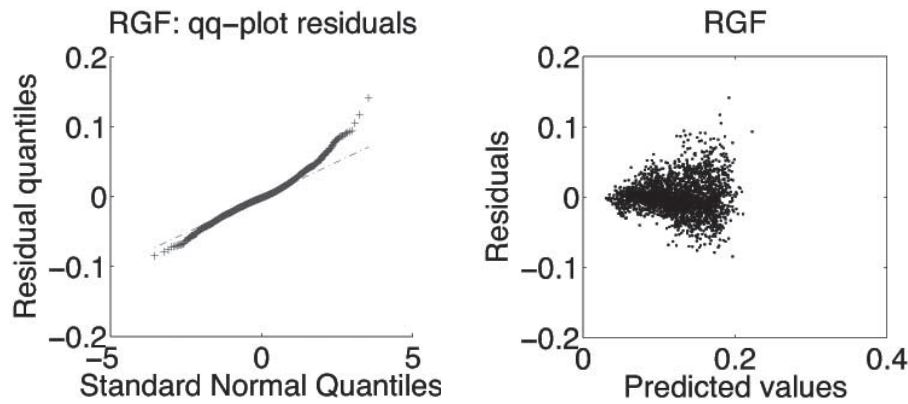


Figure 4. The residuals obtained in the estimation (Table 3) of the regression model 4: (normal) qq plot of the residuals (left) and plot of the predicted values versus the residuals (right).

Table 4. Linear relationship between the α quantiles $q_\alpha(\text{SI})$, $\alpha = 0.95, 0.975, 0.99$, and SI.

α	\hat{b}_0	\hat{b}_1	$q_\alpha(\text{SI}_{10-12})$	$q_\alpha(\text{SI}_{27-28})$
0.95	0.12761	0.00367	0.16944	0.22698
0.975	0.12920	0.00441	0.17936	0.24835
0.99	0.13248	0.00517	0.19138	0.27240

Table 5. Estimates obtained after using the estimate $\hat{K} = q_{0.975}(\text{SI}) = 0.12920 + 0.00441\text{SI}$ and fitting the RGF to the open-growth data set.

\hat{M}_0	$\hat{\lambda}$	$\hat{\delta}$
1.8×10^{-12}	0.00821	1.80736

suggested in Cronie and Särkkä (2011), and here we use the so-called *simple edge correction method* when estimating θ^* .

The estimation approach used in the present study to estimate α and μ was developed in Cronie and Yu (2010), and it is a full ML estimation scheme based on the discretely sampled *immigration-death process* (Renshaw 1994, Cronie and Yu 2010). Using this approach is equivalent to letting the natural death probability be given by $\mu + o(dt)$, hence not taking the size-dependent natural deaths into consideration. Furthermore, when this approach compares the increase/decrease of the number of trees between two consecutive time points, it does not account for the competitive deaths that have taken place. However, although it does not fully match the current model formulation, it generally performs better than the approximate ML approach of Cronie (2010) (used in Cronie and Särkkä 2011), for which the correct natural death probabilities are assumed and competitive deaths are not ignored. It manages better to take into account all the unobserved arrival/death scenarios in which trees arrive and die during the same time interval $(T_{j,k-1}, T_{j,k})$, $k = 1, \dots, n$, without being observed.

Estimation Results

Concerning the starting values used in the edge-corrected estimation procedure, the edge-corrected estimates obtained for the Scots pine data set in Cronie and Särkkä (2011) are

used as starting values for the interaction parameters c and r , i.e., $\hat{c} = 3.5$ and $\hat{r} = 4$. Moreover, because Cronie and Särkkä (2011) used the logistic growth function as an open-growth function, for the RGF part $f(\cdot; \theta)$ we choose as starting values $\hat{\delta} = -1$ and $\hat{\lambda} = 0.1$ (the latter being close to the value obtained in Cronie and Särkkä [2011]). Furthermore, the estimate $\hat{K} = q_{0.975}(\text{SI}) = 0.12920 + 0.00441 \text{SI}$ and the (known) initial size $M_0 = 0.05$ are kept fixed throughout the whole estimation. Regarding the specifics of the edge correction, for each data set we use three simulated surroundings in each iteration and then average over the estimates of the last four iterations to obtain the final estimates (see Cronie and Särkkä [2011] for details). The region on which the surrounding trees are simulated is given by a square region of side length 25 m.

In Table 6, the edge-corrected parameter estimates for all the data sets are presented. The parameter estimates for the 10 data sets are quite similar, except for plot 1, as was expected because the plots are quite similar. In the case of the open-growth parameters, we see that SI does not vary much between the plots and thus the estimates $\hat{K}(\text{SI}) = 0.12920 + 0.00441 \text{SI} \approx 0.2$ also do not vary much. The estimates of the open-growth rates λ and δ on average behave a bit differently here where there is competition present, compared with the case of the open-growth data set. In the cases in which δ is estimated to be approximately -1 ,

Table 6. Edge corrected estimates of the growth and interaction parameters together with their means and standard deviation (SD).

j	\hat{K}	$\hat{\lambda}$	$\hat{\delta}$	\hat{c}	\hat{r}	SI
1	0.18653	0.03450	0.07144	7.38389	4.25188	13
2	0.19094	0.05483	-0.47340	3.24789	3.74719	14
3	0.19976	0.08825	-0.83724	4.53837	5.92735	16
4	0.20417	0.02873	-0.46213	4.88429	5.14329	17
5	0.22181	0.08086	-0.86521	5.56370	4.57572	21
6	0.21299	0.07421	-0.83360	3.57790	2.98364	19
7	0.20858	0.05826	-0.59818	4.53696	2.57067	18
8	0.21740	0.04112	-0.35130	3.66954	4.86772	20
9	0.19094	0.06175	-0.88204	3.12824	5.35041	14
10	0.19535	0.02824	-0.75410	2.80455	3.44803	15
Mean		0.05508	-0.59858	4.33353	4.28659	
SD		0.02165	0.30408	1.38185	1.08610	

we have indications that the open-growth function behaves almost like the logistic growth function. Furthermore, when $\hat{\delta} \approx 0$ (as in the case of plot 1), we obtain an estimated open growth which, in the competitive settings of these plots, behaves approximately like the so-called Gompertz model (Lei and Zhang 2004). Note also that λ is estimated much larger than the open-growth data estimate $\hat{\lambda} = 0.00821$ in Table 5. However, this result was expected because the inclusion of competition (which inhibits the open growth) forces the open-growth rate to be higher. In addition, all estimates of δ were considerably smaller than the estimate $\hat{\delta} = 1.80736$ in Table 5, also suggesting that δ is decreased to compensate for the competition.

The estimated scale of interaction is $\hat{r} \approx 4.3$, which means that the range of the competition of a tree is estimated to be approximately 4.3 times the radius of the tree. As a result, a newly arrived tree competes for resources within a distance of approximately $\hat{r}M_0 = 4.3 \cdot 0.05 = 0.215$ m from its stem center, whereby its influence zone has size 0.145 m^2 . Similarly, for a tree at maximum size, the estimated competition distance would be approximately $\hat{r}\hat{K}(\text{SI}) \approx 4.3 \cdot 0.2 = 0.86$ m and its influence zone would have size 2.323 m^2 . For the force of interaction, the strength of the competition between a tree and its neighbor (within competing distance), i.e., the amount by which we inhibit the open growth during $(t, t + dt)$, is given by $\hat{c} \approx 4.3$ times the proportion of the tree's influence zone, which is overlapped by its neighbor's influence zone. We point out that the interaction parameters c and r (and their estimates) strongly depend on each other (Cronie and Särkkä 2011), and there is also a dependence between the open growth parameters λ and δ (and their estimates) because they both control the open-growth rate. Now, if we were to fix, say, λ and δ in the estimation, as a result the estimates of c and r would be changed/adjusted to fit the growth of the observed trees (at least to some extent). Hence, there is dependence between all parameters λ, δ, c, r .

Note further that the numerical algorithm used to minimize the sum of squares $S(\theta^*)$ stepwise samples random values for θ^* as proposed estimates and then determines whether the new proposal results in a smaller $S(\theta^*)$ than the previous minimizing θ^* does. The stopping criterion used in this stepwise procedure stops the algorithm once a threshold number of consecutive proposals without any minimization of $S(\theta^*)$ is reached. Hence, more precise estimates would possibly be obtained if this threshold were larger. However, using a larger threshold would be more time-consuming because more calculations of $S(\theta^*)$ would be needed.

We now turn to the estimates of the arrival and death rates α and μ . They can be found in Table 7. Note that they are based on the counts $n_{T_{j,1}}, n_{T_{j,2}},$ and $n_{T_{j,3}}$ in Table 1.

Assuming that the natural death probabilities are given by $\mu + o(dt)$ (immigration-death process arrivals and natural deaths) and that no trees are present at time 0, the number of trees at time $T_{j,k}$ would be Poisson distributed with parameter $\hat{\alpha}\nu(W)(1 - e^{-\hat{\mu}T_{j,k}})/\hat{\mu}$, where $\nu(W) = 10^2\pi \approx 314$ (Cronie and Yu 2010).

In the case of, e.g., plot 9 (Table 7), this translates to the estimated expected number of live trees at $T_{9,4} = 65$ being 19.4979 and, equivalently, the estimated SD of the number

Table 7. Estimates of α and μ for each plot.

j	$\hat{\alpha}$	$\hat{\mu}$
1	0.00633	0.07304
2	0.19439	2.34876
3	0.00134	0.01038
4	0.11781	2.46738
5	0.40926	2.85716
6	0.49576	4.32636
7	0.00335	0.01580
8	0.41909	2.58157
9	0.00136	0.01161
10	0.13438	2.81448
Mean	0.17831	1.75065
SD	0.19458	1.57865

of trees alive at $T_{9,4}$ being $\sqrt{19.4979} = 4.4157$. Further characteristics of $\mathbb{X}_j(T_{j,4})$, for the data sets which have a fourth inventory time, can be found in Table 8. Furthermore, to have some idea of how the data sets behave on average with respect to the number of live trees, we may use the means in Table 7 to obtain estimates of the expectation and standard deviation (SD) of the number of trees alive at, say, $T_{j,4} = 65$, and we obtain the values 31.9976 and 5.6567, respectively.

Because the GI process that we are fitting uses size-dependent natural deaths, these estimates of the behavior of the number of trees alive are not totally correct (although they are almost correct in many cases). However, by comparing the number of live trees $n_{T_{j,4}}$ at the fourth time point $T_{j,4}$ with these estimates, we gain some insight to whether the estimates $\hat{\alpha}$ and $\hat{\mu}$ are too far off. For instance, in the case of plot 9 we have that $n_{T_{9,4}} = 23$, so from the simple (approximate) prediction of 19.4979, it seems fairly acceptable. We further point out that when considering really large times $T_{j,4}$, the expected number of trees alive at $T_{j,4}$ will be approximately $\hat{\alpha}\nu(W)/\hat{\mu}$ (Cronie and Yu 2010). One may exploit this fact in future studies to improve the estimates $\hat{\alpha}$ and $\hat{\mu}$. This follows because if there is information available about the (approximate) maximum amount of trees that occupy a study region W in old Scots pine stands, we can use this maximum number (divided by the size $\nu(W)$) to estimate the ratio α/μ , and this estimate may then in turn be used as a condition/restriction when estimating α and μ .

It is likely that the estimates reported in Table 7 are quite biased because the estimation was based only on the three observations $n_{T_{j,1}}, n_{T_{j,2}},$ and $n_{T_{j,3}}$. Furthermore, it was seen in Cronie and Särkkä (2011), in the evaluation of the size-dependent estimators of Cronie (2010), that μ became heavily biased, and this further strengthens the belief that the estimates in Table 7 are biased.

Table 8. Observed and expected number of live trees, as well as stand ages, for the plots with a fourth inventory occasion.

j	2	6	8	9	10
$T_{j,4}$	42	52	43	65	65
$n_{T_{j,4}}$	52	54	36	23	16
$\hat{\alpha}\nu(W)(1 - e^{-\hat{\mu}T_{j,k}})/\hat{\mu}$	26	36	51	19.5	15

Goodness-of-Fit of the Model

Having fitted the GI process to the data, we now want to test the goodness-of-fit of the model. For this purpose measurements at a later time point $T_{j,4} > T_{j,3}$ were used as reference.

To study, among other things, the spatial structure, 999 predictions of the j th data set at its fourth sample time $T_{j,4}$ were generated by starting the simulation of the GI process with the estimated parameters in the marked point pattern at time $T_{j,3}$, $\mathbb{X}_j(T_{j,3})$, and from here running independent simulations up to the subsequent sample time point $T_{j,4}$. The observed and the simulated data at time $T_{j,4}$ were then compared by looking at empirical distributional properties of some summary statistics (by means of, e.g., Monte Carlo tests; Hope 1968).

The L function (a variance-stabilized version of Ripley's K function) and the mark-correlation function (mcf), $k(r)$ (a mean mark size scaled measure of the dependence between the mark [radius] sizes of points at a given distance r from each other) were chosen as summary statistics to describe the spatial behavior of locations and sizes (Illian et al. 2008, p. 214). In both cases, the observed summary statistics were compared with envelopes based on the predicted summary statistics (Grabarnik et al. 2011).

Stand variables typically used in forestry have also been evaluated. The first statistic considered is the *total basal area per hectare* $TBA = 10^4 \sum_i m_{i4}^2 \pi / \nu(W)$. The other three statistics are the *basal area weighted mean diameter* $WMD = \sum_i (2m_{i4})(m_{i4}^2 \pi) / \sum_i m_{i4}^2 \pi$, the mean diameter \bar{m} , and the *number of trees alive* at $T_{j,4}$, $n_{T_{j,4}}$. In Table 8, the observed and the expected number of live trees can be found for those plots that have a fourth inventory occasion. We see clearly that our predictions (expectations) tend to underestimate the number of live trees.

The results for plot 9 are as follows. The estimates of Tables 6 and 7 were used to generate the predictions, and the L function and mcf plots together with the prediction-based envelopes can be found in Figure 5.

Both in the case of the L function and the mcf, we see from Figure 5 that the curves estimated from the data clearly are inside the envelopes, and we hereby conclude, based on the spatial structure, that the point pattern and its marks can be generated by the estimated GI process. Note, however, that, in general, most data trees at time $T_{9,3}$ and $T_{9,4}$ are the same, but some new trees appear and some existing ones may die between the two time points. Moreover, it has been observed that the estimates of α and μ affect the spatial structure to a large extent.

In the case of the remaining summary statistics, the comparison of the data and the predictions can be made in the following way. Given one of the summary statistics, S , let \hat{S} denote the estimate of S based on the data and let $\hat{S}_1, \dots, \hat{S}_{999}$ denote the summary statistic estimated from the 999 predictions. To assess whether to accept the fit of the model (with respect to S), we order the 1,000 estimated summary statistics $\hat{S}, \hat{S}_1, \dots, \hat{S}_{999}$ according to their increasing sizes and check whether the *rank* (position) of \hat{S} is either very small or very large. Note that the rank can be used to formally test the fit (test statistic S) by means of Monte Carlo tests (Hope 1968, Illian et al. 2008, p. 455). In the case of $L(r)$ and $k(r)$ tests can be constructed, based on whether the estimated curves fall outside the envelopes at any distance r (maximum-minimum simultaneous/global envelopes).

In Figure 6 mark histograms for the data and one of the predictions are presented. Both have the same number of live trees.

The prediction suggests that the radii can become larger than the radii in the data (the largest tree in the prediction has radius 0.141 m and in the data it is 0.127 m). Furthermore, the radius distribution of the data has a larger proportion of smaller trees than the predictions. It seems that the estimated model either has an open growth that is too strong or the competition is too weak. Moreover, this might also suggest that $\hat{\alpha}$ should be increased to increase the number of small trees.

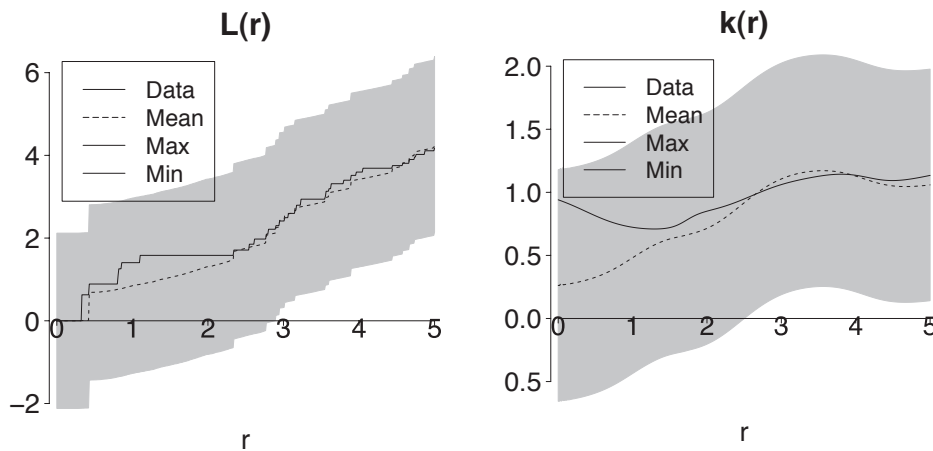


Figure 5. Left. L function, $L(r)$, for pine data set 9 at the last sample time $T_4 = T_{9,4} = 65$, together with simulated envelopes. Right. Mark correlation function, $k(r)$, for pine data set 9 at the sample time T_4 , together with simulated envelopes. The predictions (realizations) that are used to generate the envelopes are created by starting 999 simulations of the GI process in the initial state $\mathbb{X}_9(T_3)$ and, based on the parameters in Tables 6 and 7, running the simulations up to the subsequent sample time point T_4 .

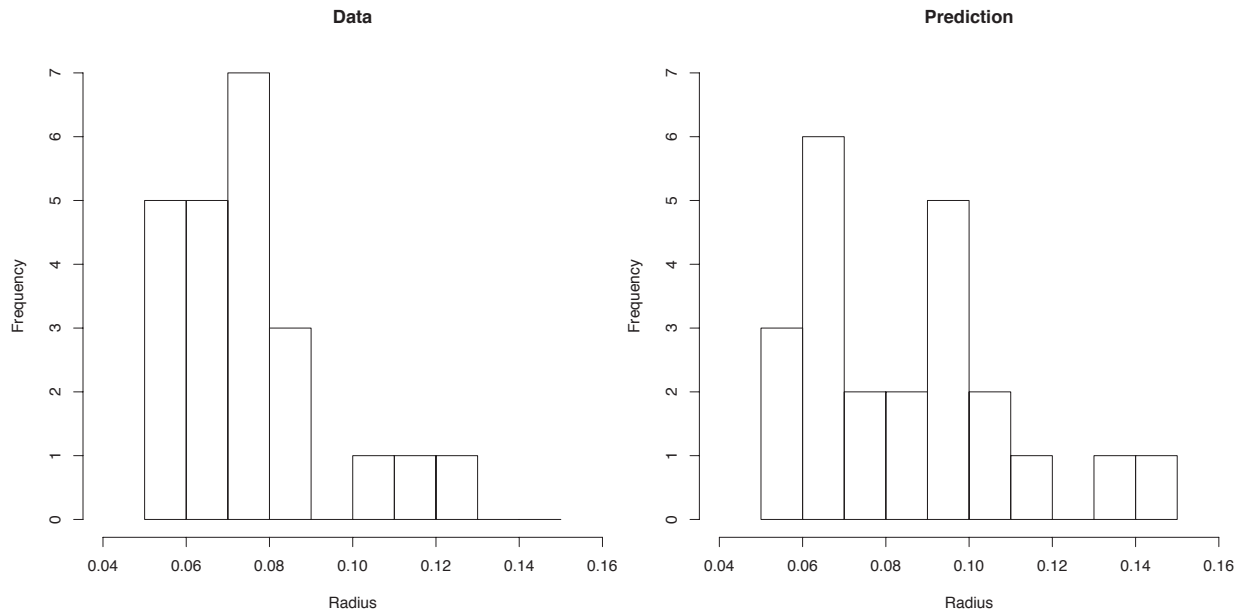


Figure 6. Radius histograms of the data (left) and a prediction (right). The prediction has the same number of live trees as the data.

To see how each tree behaves individually, we would like to measure the deviations between the actual radii and the predicted radii, for each single data tree. For a given tree i alive at $T_{9,3}$, denote by $m_{i4}^{(1)}, \dots, m_{i4}^{(999)}$ its predicted sizes at time $T_{9,4}$, and consider the corresponding residuals. Figure 7 shows the estimated mean residuals for each of the $n_{T_3} = 16$ trees that are alive at $T_{9,3}$.

It can be seen that almost all predictions are larger than zero, which confirms the overestimation of the growth. Note that because the trees in $\mathbb{X}_9(T_3)$ are already well established at T_3 , their predicted growth during the time interval (T_3, T_4) will become almost deterministic. This follows because the newcomers in (T_3, T_4) are small and by the form of the

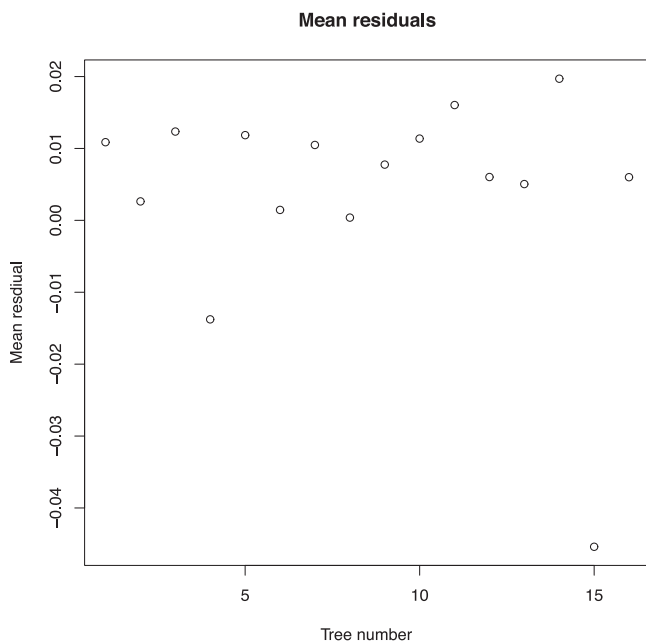


Figure 7. Mean residuals (m) for the predictions for each tree.

spatial interaction function in expression 2, small trees do not affect larger trees much. Note also that if $\hat{\mu}$ is too high, most of the predictions of a given radius m_{i4} will have $m_{i4}^{(j)} = 0$ because these predicted trees will have experienced natural deaths. During the prediction simulation, when a data tree dies, it will leave room for simulated newcomers to grow more rapidly than they would have done otherwise (because they are in a place with little interaction); therefore, the radius distribution depends on $\hat{\mu}$.

Furthermore, we see that the two trees $i = 4$ and $i = 15$ tend to always stick out, suggesting a rejection of the fit. A possible explanation for this is that these trees have small sizes and are neighbors of large trees, and because there are indications that the estimated growth is strong, it is likely that these predicted trees are killed by their predicted large neighbors.

In Table 9, we have summarized the values and the ranks of the observed summary statistics, as well as the estimated means and SDs of the predicted summary statistics.

For the total basal area TBA we cannot reject the hypothesis that the process that has generated the TBA of the forest at time T_4 and the process that has generated the TBA of the predictions (the GI process) are the same. Furthermore, as was expected, because of the radius distributions and the overprediction of the radii, the fit of the model cannot be accepted with respect to any of WMD or \bar{m} . By

Table 9. Observed summary statistics together with their ranks and the mean and SD of the predicted summary statistics.

	Observed	Rank	Mean	SD
TBA	13.63825	143	15.11195	1.43486
WMD	0.16978	1	0.20670	0.00596
\bar{m}	0.14939	1	0.18392	0.00727
n_{T_4}	23	993	16.89690	2.15259

comparing the expected number of live trees and the observed number of live trees shown in Table 8, it can be seen that they do not deviate too much from each other. However, this result indicates that the number of live trees suggested by the model is lower than its observed counterpart. Hence, either α is underestimated or μ is overestimated, and this can be redeemed by including more sample (inventory) times in the estimation of α and μ .

Conclusions

In this article, by using the open-growth data set, a linear relationship was found between the site productivity index and the large tree sizes, which provides a good approach for estimating the carrying capacity. It was shown that the performance of the Richards open growth model captures the open growth behavior for Scots pines well.

Evaluation of our growth-interaction process for spatio-temporal modeling of forest stands based on the space-time data was conducted. The preliminary results indicated that, based on the spatial structure, the point patterns and marks can be generated by the estimated GI process, according to the L function and the mark-correlation function tests. The forest stand characteristics were also evaluated. The predicted total basal area per hectare performed reasonably well but not the mean diameter or the basal area weighted mean diameter. Both of them were overestimated compared with the observed values. The estimated influence zone for an individual tree, approximately 4.3 times the tree radius, seems too small. In studies of the hampering effect of retained trees at clear felling on the development of the surrounding new regeneration, Elfving and Jakobsson (2006) reported that the volume of the new regeneration was affected up to a distance of 7 m. Further studies with extended and more heterogeneous data material are necessary to describe the competition among the trees within the stand. Marked point pattern analyses combined with indicators of spatial autocorrelations (Shi and Zhang 2003) might provide useful information to mimic the competition effect in the model. The number of stems in the plots for which we have made predictions was underestimated, except for one plot. For unknown reasons the observed mortality (death rate) between the third and the fourth inventory times was unusually high on that plot.

Discussion

Because the estimates of the GI model parameters depend on the expected tree population size at a given time point, a starting point in our continuing work will be to further investigate the arrival and death process. Hereby, it is also required that we have more frequently sampled data. We have chosen to model the tree population with a rbh ≥ 5 cm because we have complete spatial information for these trees. Note that today's forestry focuses on low death rate scenarios and rather regular spatial arrangements of established seedlings, which differs from naturally regenerated forests. Additional information about potential arrivals (i.e., trees < 5 cm rbh) at a given time point would probably improve the model evaluation and development. The trees

in the space-time data set in the present study are all rather young at the first inventory time with a large amount of new arrivals exceeding the threshold diameter (5 cm rbh). To better describe and capture the development of pine stands during the whole life cycle, the data must be supplemented with older stands.

We have already mentioned a possible bias in the estimates of α and μ , which is a consequence of the few (three) sample times in the data, and because these estimates influence how the 999 simulations used in the goodness-of-fit testing are generated, a comment related to possible robustness issues is in place. Considering the conditional SD of the number of trees present at $T_{9,4}$, given $n_{T_{9,3}}$, which is provided by (Cronie and Yu 2010)

$$\begin{aligned} \sigma(\alpha, \mu) &= \sqrt{(1 - e^{-\mu(T_{9,4}-T_{9,3})}) \left(n_{T_{9,3}} e^{-\mu(T_{9,4}-T_{9,3})} + \frac{\alpha}{\mu} \right)} \\ &= \sqrt{(1 - e^{-9\mu}) \left(16e^{-9\mu} + \frac{\alpha}{\mu} \right)}, \end{aligned}$$

it is clear that the radius distributions and thereby the mean marks of the simulations are influenced by the estimate $\hat{\sigma} = \sigma(\hat{\alpha}, \hat{\mu})$. Moreover, the L function and mcf estimates used in computing the envelopes in Figure 5 depend on the spatial structure of the 999 simulations used. Because the number of trees present in a simulation influences its spatial structure (recall the comment about the influence of $\hat{\alpha}$ and $\hat{\mu}$ on the spatial structures), there is a chance that $\hat{\sigma}$ has an influence on the shape of the envelopes and thereby on conclusions drawn about the fit of the model. To give an idea of how strong these influences may be, we observe that $\hat{\sigma} = 1.20066$ when the estimates $(\hat{\alpha}, \hat{\mu}) = (0.00136, 0.01161)$ are used. By increasing $\hat{\alpha}$ to even $100\hat{\alpha} = 0.136$ (compensation for possible underestimation), we obtain $\hat{\sigma} = 1.61002$ (34% increase); therefore, the prediction of $\hat{n}_{T_{9,4}}$ is fairly robust with regard to an increase in $\hat{\alpha}$. If we instead decrease $\hat{\mu}$ to $\hat{\mu}/2 = 0.005805$ (compensation for possible overestimation), however, we obtain $\hat{\sigma} = 0.88596$ (0.26% decrease) whereby we see that $\hat{\sigma}$ and thus the estimated population size are more sensitive (less robust) to changes in $\hat{\mu}$ (when both changes are carried out simultaneously, we obtain $\hat{\sigma} = 1.40199$). In terms of the envelopes, an increase in $\hat{\alpha}$ should produce wider envelopes, whereas a decrease in $\hat{\mu}$ would create more narrow envelopes. Hence, a bias in $(\hat{\alpha}, \hat{\mu})$ (which is most likely present) will have an effect on the goodness-of-fit tests used. However, although the uncertainty in the conclusions drawn about the fit of the model would be decreased significantly if more temporal instances were available in the data, the possible bias in $(\hat{\alpha}, \hat{\mu})$ may not play a decisive role in the assessment of the fit of the model.

Literature Cited

- COMAS, C. 2009. Modelling forest regeneration strategies through the development of a spatio-temporal growth interaction model. *Stochas. Env. Res. Risk Assess.* 23:1089–1102.
- CRONIE, O. 2010. *Some edge correction methods for marked spatio-temporal point process models*. Preprint 2010:9. Mathematical Sciences, Chalmers University of Technology and University of Gothenburg. 39 p. Available online at www.

- math.chalmers.se/Math/Research/Preprints/2010/9.pdf; last accessed Aug. 1, 2012.
- CRONIE, O., K. NYSTRÖM, AND J. YU. 2011. *Spatio-temporal modelling of Swedish Scots pine stands*. Research Report 2011:03. Centre of Biostochastics, Swedish University of Agricultural Sciences. 30 p. Available online at biostochastics.slu.se/publikationer/dokument/Report201103.pdf; last accessed Aug. 1, 2012.
- CRONIE, O., AND A. SÄRKKÄ. 2011. Some edge correction methods for marked spatio-temporal point process models. *Comput. Stat. Data Anal.* 55:2209–2220.
- CRONIE, O., AND J. YU. 2010. *Maximum likelihood estimation in a discretely observed immigration-death process*. Research Report 2010:1. Centre of Biostochastics, Swedish University of Agricultural Sciences. 56 p. Available online at biostochastics.slu.se/publikationer/dokument/Report2010_01.pdf; last accessed Aug. 1, 2012.
- DIGGLE, P. 2003. *Statistical analysis of spatial point patterns*, 2nd ed. Oxford University Press, Oxford, UK. 168 p.
- ELFVING, B., AND R. JAKOBSSON. 2006. Effects of retained trees on tree growth and field vegetation in *Pinus sylvestris* stands in Sweden. *Scand. J. For. Res.* 21(Suppl. 7):29–36.
- GERRARD, D.J. 1969. *Competition quotient—A new measure of the competition affecting individual forest trees*. Mich. State Univ., Agr. Exp. Station Res. Bull. 20. 32 p.
- GRABARNIK, P., M. MYLLYMÄKI, AND D. STOYAN. 2011. Correct testing of mark independence for marked point patterns. *Ecol. Model.* 222:3888–3894.
- GRABARNIK, P., AND A. SÄRKKÄ. 2009. Modelling the spatial structure of forest stands by multivariate point processes with hierarchical interactions. *Ecol. Model.* 220:1232–1240.
- GRATZER, G., C. CANHAM, U. DIECKMANN, A. FISCHER, Y. IWASA, R. LAW, M.J. LEXER, ET AL. 2004. Spatio-temporal development of forests—Current trends in field methods and models. *Oikos* 107(1):3–15.
- HÄGGLUND, B., AND J.E. LUNDMARK. 1977. Site index estimation by means of site properties. Scots pine and Norway spruce in Sweden. *Stud. For. Suec.* 138:5–38.
- HOPE, A.C.A. 1968. A simplified Monte Carlo significance test procedure. *J. Roy. Stat. Soc. B* 30:582–598.
- ILLIAN, J., A. PENTTINEN, H. STOYAN, AND D. STOYAN. 2008. *Statistical analysis and modelling of spatial point patterns*. Wiley-Interscience, New York. 560 p.
- LEI, Y.C., AND S.Y. ZHANG. 2004. Features and partial derivatives of Bertalanffy-Richards growth model in forestry. *Nonlinear Anal. Model. Control* 9:65–73.
- NORD-LARSEN, T. 2006. Modeling individual-tree growth from data with highly irregular measurement intervals. *For. Sci.* 52:198–208.
- PRÉVOSTO, B., T. CURT, J. GUEUGNOT, AND P. COQUILLARD. 2000. Modeling mid-elevation Scots pine growth on a volcanic substrate. *For. Ecol. Manage.* 131:223–237.
- PUKKALA, T., T. KOLSTRÖM, AND J. MIINAA. 1994. A method for predicting tree dimensions in Scots pine and Norway spruce stands. *For. Ecol. Manage.* 65:123–134.
- RANNEBY, B., T. CRUSE, B. HÄGGLUND, H. JONASSON, AND J. SWÄRD. 1987. Designing a new national forest survey for Sweden. *Stud. For. Suec.* 177:1–29.
- RENSHAW, E. 1994. The linear spatial-temporal interaction process and its relation to $1/\omega$ -noise. *J. Roy. Stat. Soc. B* 56:75–91.
- RENSHAW, E., AND C. COMAS. 2009. Space-time generation of high intensity patterns using growth-interaction processes. *Stat. Comput.* 19:423–437.
- RENSHAW, E., C. COMAS, AND J. MATEU. 2009. Analysis of forest thinning strategies through the development of space-time growth-interaction simulation models. *Stochas. Env. Res. Risk Assess.* 23:275–288.
- SÄRKKÄ, A., AND E. RENSCHAW. 2006. The analysis of marked point patterns evolving through space and time. *Comput. Stat. Data Anal.* 51:1698–1718.
- SEBER, G., AND C. WILD. 1989. *Nonlinear regression*. John Wiley and Sons, New York. 800 p.
- SHI, H.J., AND L.J. ZHANG. 2003. Local analysis of tree competition and growth. *For. Sci.* 49(6):938–955.
- SHIFLEY, S.R., AND G.J. BRAND. 1984. Chapman-Richards growth function constrained for maximum tree size. *For. Sci.* 30(4):1066–1070.
- SMITH, W.R., R.R. FARRAR JR., P.A. MURPHY, J.L. YEISER, R.S. MELDAHL, AND J.S. KUSH. 1992. Crown and basal area relationships of open-growth southern pines for modeling competition and growth. *Can. J. For. Res.* 22:341–347.
- SÖDERBERG, U. 1997. Country report for Sweden. P. 955–1017 in *Study on European forestry information and communication system. Reports on forestry inventory and survey systems*, vol. 2, Päivinen, R., and M. Köhl (eds.). Office for Official Publications of the European Communities, Luxembourg.
- STOYAN, D., AND A. PENTTINEN. 2000. Recent applications of point process methods in forestry statistics. *Stat. Sci.* 15:61–78.
- VOSPERNIK, S., R.A. MONSERUD, AND H. STERBA. 2010. Do individual-tree growth models correctly represent height:diameter ratios of Norway spruce and Scots pine? *For. Ecol. Manage.* 260:1735–1753.
- WEINER, J., AND C. DAMGAARD. 2006. Size-asymmetric competition and size-asymmetric growth in a spatially explicit zone-of-influence model of plant competition. *Ecol. Res.* 21:707–712.
- ZEIDE, B. 1993. Analysis of growth equations. *For. Sci.* 39:594–616.

Reproduced with permission of the copyright owner. Further reproduction prohibited without permission.